A Side Reaction of Alanine Racemase: Transamination of Cycloserine[†,‡]

Timothy D. Fenn,[&,#] Geoffrey F. Stamper,[§,||,#] Anthony A. Morollo,[&,⊥] and Dagmar Ringe*[,&,§]

Department of Biochemistry and Chemistry, and Program in Biophysics and Structural Biology, Rosenstiel Basic Medical Sciences Research Center, Brandeis University, Waltham, Massachusetts 02454

Received October 17, 2002; Revised Manuscript Received February 10, 2003

ABSTRACT: Alanine racemase (EC 5.1.1.1) catalyzes the interconversion of alanine enantiomers, and thus represents the first committed step involved in bacterial cell wall biosynthesis. Cycloserine acts as a suicide inhibitor of alanine racemase and as such, serves as an antimicrobial agent. The chemical means by which cycloserine inhibits alanine racemase is unknown. Through spectroscopic assays, we show here evidence of a pyridoxal derivative (arising from either isomer of cycloserine) saturated at the C4′ carbon position. We additionally report the L- and D-cycloserine inactivated crystal structures of *Bacillus stearothermophilus* alanine racemase, which corroborates the spectroscopy via evidence of a 3-hydroxyisoxazole pyridoxamine derivative. Upon the basis of the kinetic and structural properties of both the L- and D-isomers of the inhibitor, we propose a mechanism of alanine racemase inactivation by cycloserine. This pathway involves an initial transamination step followed by tautomerization to form a stable aromatic adduct, a scheme similar to that seen in cycloserine inactivation of aminotransferases.

The L-isomers of amino acids are commonly found in nature and produced through a variety of biosynthetic pathways (*1*). However, formation of their enantiomeric mates typically requires some form of chiral reduction (e.g., D-amino acid aminotransferase (D-aAT),[1] EC 2.6.1.21) or an enzymatically catalyzed equilibration about the α-carbon between the two isomers. Alanine racemase catalyzes the latter, and in bacterial species generates D-alanine, a constituent of the peptide linker found in the peptidoglycan layer of the cell wall (*1*, *2*).

Alanine racemase utilizes pyridoxal 5′-phosphate (PLP) to carry out racemization. The reaction is initiated by Schiff base formation between substrate and cofactor (a common step among all PLP-dependent transformations), following which the substrate α-carbon can be deprotonated and stabilized through electron delocalization via the electrophilic pyridinium nitrogen. The resulting carbanion can then undergo one of a number of mechanistic fates including racemization, transamination, and various elimination reactions (*3*). In the case of alanine racemase, the presence of two bases (Lys39 and Tyr265′[2]) on either side of the pyridinium ring in an antiparallel configuration suggests a means for "steering" the chemistry down the racemization path as opposed to one of many other possible PLP-catalyzed pathways (*4*, *5*). In the racemase mechanism, Lys39 and Tyr265′ act as the conjugate acid/base pair.

Cycloserine (4-amino-3-isoxazolidinone) is a naturally occurring inhibitor of PLP-dependent enzymes. In either the natural D- or synthetic L-isomer form, cycloserine acts as an essentially irreversible inhibitor of many PLP-dependent enzymes, including alanine racemase (*6*−*8*). More recent studies using D-aAT inactivated with D-cycloserine (PDB ID 2DAA) suggest a mechanism of inactivation that results in aromatization of the parent compound (Scheme 1) (*9*). This mechanism requires an initial transamination step (proton transfer from the substrate C2 to cofactor C4′), forming an exocyclic ketimine that is no longer conjugated with the pyridine ring. This ketimine can then proceed through a second prototropic shift, forming a stable covalent adduct. NMR and IR spectra indicate cycloserine exists in solution primarily in the lactim form, which affords the second tautomerization by sufficiently decreasing the β proton pK_a to allow for the required acid−base chemistry to occur (*9*).

Reaction of dialkylglycine decarboxylase (EC 4.1.1.64) with L- or D-cycloserine follows a different reaction pathway dependent upon inhibitor chirality, resulting in two chemically different products (PDB IDs 1D7U and 1D7S, respectively). While both isomers are competitive inhibitors, the crystallographic structures of the enzyme−cycloserine complexes reveal sp^3 geometry at the C_α for D-cycloserine and sp^2 geometry at the C_α for L-cycloserine cofactor adducts (*10*). If cycloserine binds to the enzyme in the same configuration as substrate, this difference in reactivity can be attributed to the absence of a sufficient base for α-proton abstraction in the case of D substrates, for which the α-proton

[†] This work was supported by a grant from the Molecular and Cellular Biosciences Division of the National Science Foundation.

[‡] Coordinates have been deposited in the RCSB Protein Data bank (http://www.rcsb.org) under the accession code 1EPV (DCS) and 1NIU (LCS).

* Corresponding author. E-mail: ringe@brandeis.edu.

[&] Department of Biochemistry and Chemistry.

[§] Program in Biophysics and Structural Biology.

[#] These authors contributed equally to this work.

[||] Current address: Abbott Laboratories, Abbott Park, IL.

[⊥] Current address: GPC Biotech, Inc. 610 Lincoln Street, Waltham, MA 02451.

[1] Abbreviations: D-aAT, D-amino acid aminotransferase; CD, circular dichroism; CHES, 2-(*N*-cyclohexylamino)ethanesulfonic acid; NAD^+, β-nicotinamide adenine dinucleotide; PEG, poly(ethylene glycol); PLP, pyridoxal 5′-phosphate; PMP, pyridoxamine 5′-phosphate.

[2] Residues marked with a prime are donated by the opposing monomer in the dimer.

10.1021/bi027022d CCC: $25.00 © 2003 American Chemical Society
Published on Web 04/23/2003

Scheme 1: Current Mechanism of Inactivation of Aminotransferases by Cycloserine[a]

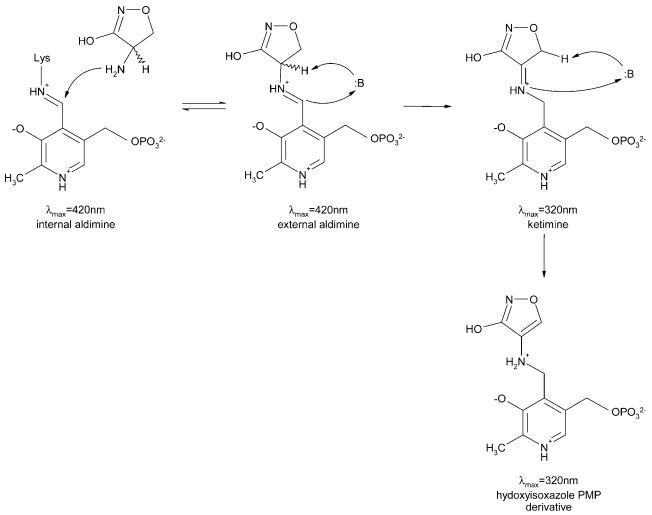

[a] Also shown are approximate absorbance maxima of each species. Proton transfers are drawn as concerted mechanisms for the sake of brevity.

is facing solvent, and therefore the sp^3 character of the bound substrate is preserved. In the case of the L-isomer, the α-proton is directed toward the active site lysine, the base responsible for the prototropic shift which results in the exocyclic ketimine—thus resulting in sp^2 geometry at the α-carbon of cycloserine. However, this ketimine does not undergo the second prototropic shift observed with D-aAT to form an aromatic adduct.

The cycloserine studies presented thus far require forms of PLP chemistry not typical of alanine racemase. However, studies by Kurokawa et al. have shown transamination is observed once in every 10^7 turnovers (*11*). Consequently, inactivation of alanine racemase by cycloserine could proceed via transamination as detailed above. The impressive partitioning between racemization and transamination is a suggested result of the antiparallel two base system. Additionally, the presence of a putative low barrier hydrogen bond between Arg219 and the pyridinium nitrogen of the PLP ring may not only facilitate carbanion formation, but may somehow be linked to reaction specificity (*12*, *13*).

Studies of *B. stearothermophilus* alanine racemase with several suicide substrates (including L- and D-cycloserine) indicate a marked difference in inactivation rates between the two isomers upon incubation with the enzyme (*8*). This finding may have some relationship to the one base inhibition mechanism for dialkylglycine decarboxylase, in that alanine racemase may only be capable of inactivation through one of the two catalytic bases while the second follows a different pathway or is impeded in some fashion. The support for this hypothesis lies in the seemingly ubiquitous number of PLP-dependent enzymes that employ a one base mechanism to achieve transamination (*3*). Alternatively, the differences in rates may be due to intrinsic differences in the two catalytic bases in the case of alanine racemase (*5*).

The goal of this study has been to determine the inactivation mechanism of cycloserine as it pertains to *B. stearothermophilus* alanine racemase. Specifically, our interest lies in determining whether alanine racemase does indeed follow the aforementioned inhibition scheme of initiating transamination followed by inactivation; if so, we have sought to determine which residues act in this role, and how this may explain the oft-observed difference in reactivity between enantiomers (*8*). We have shown through the combination of X-ray crystallographic and spectroscopic methods that alanine racemase is inactivated by cycloserine through a mechanism of inactivation similar to that of D-aAT, but requires different mechanisms dependent upon the initial stereochemistry of cycloserine. The studies also suggest a role for the active site residue Tyr265 in controlling the reactivity of the PLP cofactor in addition to acting as a catalytic base.

MATERIALS AND METHODS

Materials. D-Cycloserine, D-alanine, L-alanine dehydrogenase, and NAD^+ were purchased from Sigma (St. Louis, MO). CHES buffer and PEG 4K were purchased from Fluka (St. Louis, MO). L-Cycloserine was purchased from Jannsen Chemical.

Protein Purification. B. stearothermophilus alanine racemase was prepared as described previously (*14*). Purified enzyme was run over a Bio-Gel P-6DG (Bio-Rad) column (*2* × 45 cm) using 100 mM Tris-HCl buffer (pH 8.5) containing 0.01% 2-mercaptoethanol and 10 μM PLP as eluent. Protein was concentrated using Amicon concentrators with a 10 kDa molecular mass cutoff.

Crystallization. Alanine racemase crystals (0.5 × 0.5 × 0.3 mm) were grown by the hanging drop method using purified enzyme concentrated to 22 mg/mL. The hanging drop contained 10 μL of the protein solution, 10 μL of 23% (w/v) PEG 4K, 200 mM sodium acetate, and 100 mM Tris (pH 8.5). Drops were equilibrated against 700 μL of the PEG 4K solution. As described previously (*14*, *15*), the crystals have a distinct yellow color due to the presence of PLP in an aldimine linkage. Stock solutions of 100 mM L- and D-cycloserine were prepared using the same components in the well solution. A 2 μL volume of the hanging drop was removed and replaced with the inhibitor solution every 20 min for 4 h. The crystals lost the yellow color within the first 30 min of buffer exchanges.

Data Collection and Processing. The diffraction data were collected at room temperature using Cu Kα radiation generated by an in-house Rigaku 300B rotating anode X-ray generator running at 40 kW × 30 mA. The diffraction images were recorded using an RAXIS−IV image plate detector. All diffraction data were integrated, scaled, and merged using the HKL software package (*16*). The crystals have symmetry $P2_12_12_1$, and contain one dimer per asymmetric unit. The data processing results for both data sets are outlined in Table 1.

Structure Solution and Refinement. Crystals of both inhibitor−enzyme complexes were reasonably isomorphous with the crystal used in the determination of the native structure reported by Shaw et al. (*15*), and therefore the native structure as a dimer was used as the starting model, with the PLP cofactor, acetate and water molecules removed from the original coordinate file (PDB ID 1SFT). All refinement procedures were done using the software package CNS (*17*). Model and refinement statistics are listed in Table 1.

Application of phases calculated from the original coordinates resulted in initial crystallographic *R*-factors of 0.31

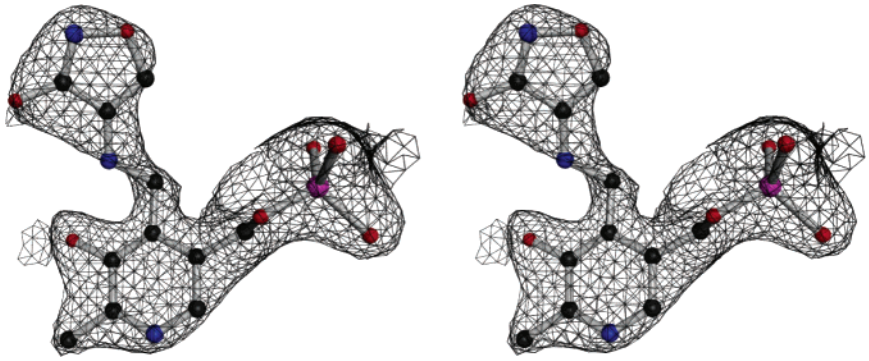

FIGURE 1: Stereoview of σ_A-weighted simulated annealing omit maps in which all atoms shown were omitted from the Fourier synthesis. Maps are shown at 1.0 σ for the L-cycloserine adduct only, as the D-cycloserine maps appear similar. This figure was generated with POVScript+ (http://www.brandeis.edu/~fenn/povscript) and rendered with POVRay (http://www.povray.org).

Table 1: Crystallographic Data and Model Statistics

	L-cycloserine	D-cycloserine
data collection		
space group	$P2_12_12_1$	$P2_12_12_1$
unit cell		
a (Å)	99.16	98.59
b (Å)	90.24	89.94
c (Å)	85.26	85.17
resolution range (Å)	20−2.2	20−2.0
no. of observations	218570	315226
no. of unique reflections	39472	60403
R_{merge}[b] (%)	8.4	7.5
completeness, overall (%)	90.8	91.8
completeness, outer shell[c]	92.3	56.8
refinement statistics		
resolution range [$F/\sigma(F) > 0$; Å]	20−2.2	20−2.0
no. of reflections	31194	47531
R_{factor}[d] (%)	20.8	21.7
R_{free}[e] (for 2340 and 1907 reflections; %)	23.1	23.5
no. of protein atoms	6059	6049
no. of cycloserine-PLP atoms	44	44
no. of water molecules	254	188
RMSD from ideality		
bond lengths (Å)	0.02	0.01
bond angles (deg)	2.5	2.1
improper angles (deg)	1.7	1.5
dihedral angles (deg)	25.9	25.6

[a] Unique reflections where $(I/\sigma(I) > 0)$. [b] $R_{merge} = \Sigma|I_{obs} - I_{avg}|/\Sigma I_{obs}$. [c] Outer shells are 2.28−2.20 Å, 1.97−1.90 Å for L-cycloserine and D-cycloserine, respectively. [d] $R_{factor} = \Sigma||F_{obs}| - |F_{calc}||/\Sigma|F_{obs}|$, where F_{obs} is the observed structure factor amplitude and F_{calc} is the calculated structure factor amplitude. [e] See Brunger (*25*) for a description of R_{free}.

(R_{free} of 0.31) and 0.28 (R_{free} of 0.27) for the L- and D-cycloserine complex structures, respectively. The starting models were then subjected to rigid body refinement. Reflections in the 20−4.0 Å resolution range were used for both the L-cycloserine (5368 reflections) and D-cycloserine (6349 reflections) complex structures. The rigid body refinement procedure, where each monomer was treated individually, lowered the crystallographic *R*-factor to 0.27 (R_{free} 0.28) and 0.27 (R_{free} 0.26) for the L- and D-cycloserine complex structures. Subsequent rounds of positional refinement were carried out on each structure. For the L-cycloserine complex, the final positional refinement procedure in the initial round used all the reflections in the resolution range of 20−2.2 Å (30 280 reflections). This round of refinement yielded an *R*-factor of 0.25 and a free *R*-factor of 0.27. Difference electron density maps with coefficients $2F_{obs}-F_{calc}$ and $F_{obs}-F_{calc}$ (*18*, *19*) were calculated at this stage in the refinement, providing interpretable electron density for a covalent cofactor derivative in the active site. The electron density at the active site was consistent with a planar cycloserine ring (sp^2 hybridized C_α) and a sp^3 hybridized C4′ carbon on the PLP cofactor (Figure 1). A model of the cofactor derivative was built using the program INSIGHT (Molecular Simulations, Inc.) and the coordinates were added to the protein model. Water molecules that were observed in the original native structure (PDB ID 1SFT) and whose electron density was observed at these positions in the current structures were added to the models. These new models were then subjected to further rounds of positional refinement as well as overall and individual B-factor refinement procedures.

Additional water molecules were located and added to the models using the WATERPICK procedure in the CNS program package. Refinement and model quality statistics for the complex structures are summarized in Table 1. The final models were analyzed using PROCHECK. For the L-cycloserine inhibited structure, PROCHECK determined that 91.7% of all the residues were in the most favored regions on a Ramachandran plot, 7.8% of the residues were in additional allowed regions, and 0.4% of the residues were in generously allowed regions. For the D-cycloserine inhibited structure, PROCHECK determined that 92.2% of all the residues were in the most favored regions of a Ramachandran plot, 7.2% of the residues were in additional allowed regions, and 0.6% of the residues were in generously allowed regions. No residues were found in disallowed regions for either structure.

A series of simulated annealing omit maps (*20*), in which 15 residue segments were systematically omitted throughout the entire chain of each monomer, were calculated to find large conformational changes or rearrangements in the overall fold. No such rearrangements were found in the structures and there is interpretable electron density for most of the protein. However, there are some surface residues where the electron density is poor or absent.

Enzyme Assays. Enzyme activity was followed in the D → L direction by monitoring the increase in NADH at 340 nm in a coupled assay with L-alanine dehydrogenase (*8*). An extinction coefficient for NADH at 340 nm of 6220 M^{-1} cm^{-1} was assumed. All reactions were carried out at 37 °C. The assays were performed using 1 mL of 100 mM CHES buffer (pH 9.1) containing 5 mM NAD^+, 3 units of L-alanine dehydrogenase (1 unit converts 1 μmol of L-alanine to pyruvate and NH_3 per minute at pH 10 and 25 °C) and 100

mM D-alanine. The reaction was initiated by adding the desired amount of enzyme.

UV−Vis Spectroscopy. Samples of purified alanine racemase (1.27 mg/mL) at 25 °C in 100 mM Tris buffer (pH 8.5) containing 0.01% 2-mercaptoethanol were used in all spectroscopic assays. Inactivation reactions were initiated through the addition of the desired amount of either L- or D-cycloserine. Absorbance changes at 420 nm were recorded every second for 3 min and plotted vs time. For each isomer, inactivation rates (k_2) were determined from double reciprocal plots according to eq 1.

$$E + I \underset{k_{-1}}{\overset{k_1}{\rightleftharpoons}} E{\cdot}I \xrightarrow{k_2} E{\cdot}X \quad (1)$$

In all experiments, [I] ≫ E such that pseudo first-order behavior was observed. Additionally, spectra of the samples, using a broad wavelength range (300−550 nm), were recorded at 1-min intervals for 20 min upon incubation with cycloserine using a Hewlett-Packard UV−Vis diode array spectrophotometer. All reactions were referenced against a cell containing protein in the absence of inactivator.

Time Dependent Inactivation. Inactivation of alanine racemase by L- or D-cycloserine was determined by incubating the enzyme (696 nM) with varying concentrations of either enantiomer of cycloserine. The inactivation reaction was quenched by diluting the enzyme−inhibitor mixture 100-fold into ice-cold 100 mM Tris buffer (pH 8.5) containing 0.01% 2-mercaptoethanol. A total of 50 μL of this solution was then used in the activity assay. In each experiment, the enzyme was incubated until the remaining activity was equal to or less than 50% of the original. Two activity measurements were taken at each time interval. The resulting average remaining activities were then plotted versus time. For each isomer, the limiting inactivation rate was determined from a double reciprocal plot as per eq 1.

Circular Dichroism. The racemization of either enantiomers of alanine or cycloserine was tested by incubating the desired substrate (5 mM for alanine, 10 mM for cycloserine) at 25 °C in 50 mM borate (pH 9.1) containing 100 mM KCl, and recording the CD signal (at 215 nm for alanine, 264 nm for cycloserine) as a function of time. Reactions were initiated by the addition of enzyme (0.015 and 0.046 mg/mL for alanine, 0.15 mg/mL for cycloserine). Wavelength scans (200−350 nm) were also performed before and after the completion of each reaction.

RESULTS AND DISCUSSION

Alanine racemase has adopted a structural configuration that allows for a highly specific reaction chemistry (*11*), leading to racemization over other transformations that can be catalyzed by PLP. Therefore, it seems unusual that a transamination-based inactivator would have a reasonable effect on this racemase (*8*). Also, the observation that the two isomers react at different rates implies a like conclusion to that of dialkylglycine decarboxylase; substrate chirality may dictate the pathway of inactivation. The mechanism of inactivation of alanine racemase by L- and D-cycloserine has been studied both structurally and kinetically. The structures provide the form of the inactivated protein, thereby defining the type of chemistry that must occur at the active site. The kinetics of inactivation provide information about the efficiency of this process for either isomer. Taken together, a mechanism for the overall reaction can be proposed.

Cycloserine−Enzyme Complex Structures. To directly observe the inactivated enzyme, we determined the crystal structures of the L-cycloserine complex to 2.2 Å resolution and the D-cycloserine complex to 2.0 Å. The presence of the cofactor derivative in the active site of either structure does not induce any conformational changes in the enzyme. The rms deviations between the native (*15*) and the cycloserine−enzyme complex structures are 0.06 and 0.04 Å (C_α) and 0.21 and 0.19 Å (non-hydrogen atoms), for the L- and D-cycloserine structures, respectively. In each structure, the electron density of the cofactor derivative is consistent with a closed planar ring and a saturated C4′ carbon (Figure 1). Consequently, the model was built as a 3-hydroxyisoxazole PMP derivative and the appropriate parameters were used for the refinement.

The electron density for Tyr265 is partially disordered in the D-cycloserine−enzyme complex structure, making positioning of the residue difficult. The modeled position is based on the density observed for the beta and gamma carbons indicating the directionality of the ring. Disordered density for Tyr265 has been observed before in both the native (*15*) and the propionate complex (*14*) structures. In addition, it appears from the electron density that the nearby Cys311′ samples multiple distinct conformations, which may be contributing to the disorder of the tyrosine side chain. In its current position, the phenolic oxygen of Tyr265 is approximately 3.0 Å from the C_α atom of the isoxazole ring, 3.2 Å from the PMP nitrogen and 4.2 Å from the C4′ carbon.

The cofactor derivative is held in the active site by a network of hydrogen bonds similar to those found in all the structures reported for this enzyme (Figures 2 and 3). A carboxylate binding motif has been observed in structures of alanine racemase in complex with acetate (*15*), propionate (*14*), and both the L- and D-isomers of alanine phosphonate (*4*, Stamper, unpublished results). This same binding motif is observed in both cycloserine−enzyme complex structures interacting with the hydroxy imine that forms part of the hydroxyisoxazole ring. The hydroxyl moiety interacts with Arg136, Tyr265, and an active site water molecule, while the nitrogen interacts with the backbone amide of Met312′ and the same active site water molecule.

Inactivation of D-aAT with cycloserine produces the same derivative of PLP as seen here with alanine racemase. The formation of identical product complexes for alanine racemase and D-aAT provides evidence for a transimination reaction inherent in PLP-catalyzed transaminase activity (*9*). This capability has been demonstrated previously using an indirect assay involving tritium release from [4′-^{3}H]PMP incubated with apo alanine racemase (*11*, *21*). In the specific case of cycloserine, transimination must then be followed by irreversible tautomerization of the ketimine to form a stable isoxazole (Scheme 1), as seen in the planarity of the cycloserine ring and sp^3 hybdridization on C4′ (Figure 1). Also, the initial proton transfer from substrate C_α to cofactor C4′ occurs irrespective of initial inhibitor chirality, a phenomenon not seen in dialkylglycine decarboxylase (*10*). This suggests that either both Lys39 and Tyr265 are capable of carrying out the aldimine to ketimine conversion, or that only one base is capable of the transimination reaction and

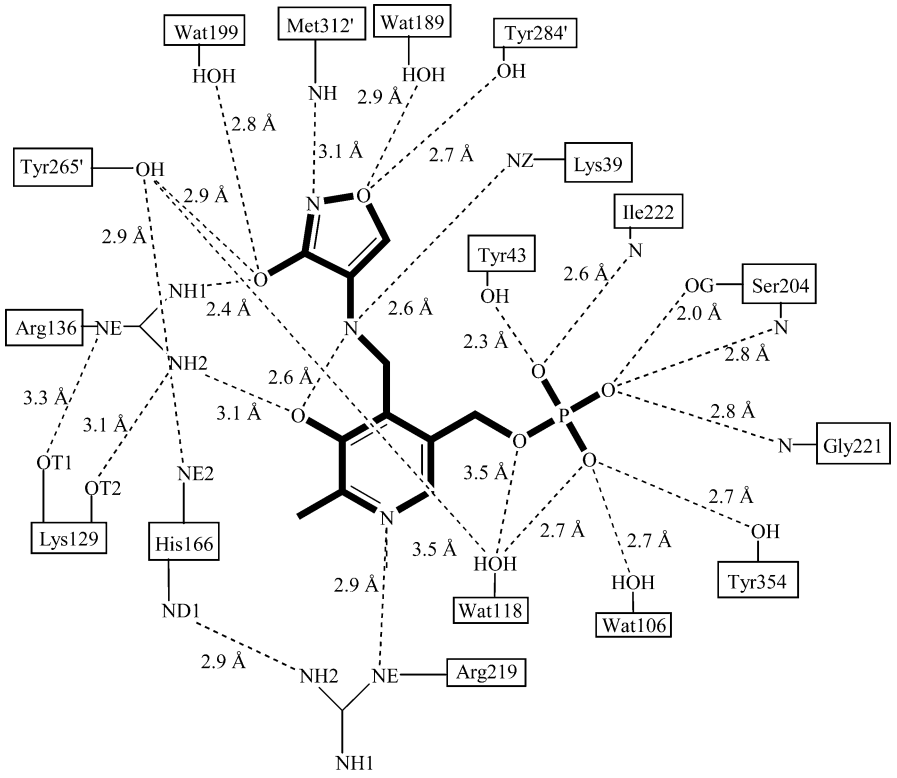

FIGURE 2: Schematic diagram showing the interactions between the 3-hydroxyisoxazole PMP derivative derived from L-cycloserine and the amino acids and water molecules in the active site. Prime labels indicate residues donated by the other subunit in the dimer. Atoms labeled are in PDB format.

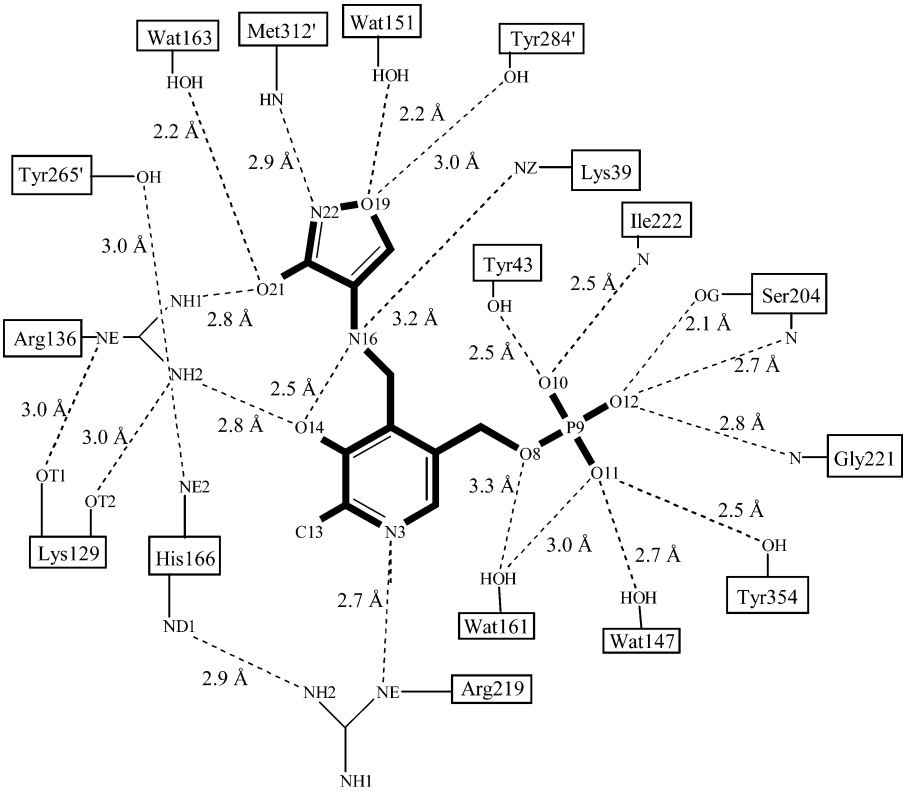

FIGURE 3: Schematic diagram showing the interactions between the 3-hydroxyisoxazole PMP derivative derived from D-cycloserine and the amino acids and water molecules in the active site. Prime labels indicate residues donated by the other subunit in the dimer. Atoms labeled are in PDB format.

racemization to a specific enantiomer is required prior to this step. In either case, both bases are required to inactivate the enzyme; only the mechanistic role each base performs in the two possibilities is different. These models are in contrast to the currently available, single-base-catalyzed cycloserine inactivation mechanism for PLP-dependent enzymes (Scheme 1) (*8*−*10*). Therefore, spectral and time-dependent inactivation analyses were carried out to elucidate

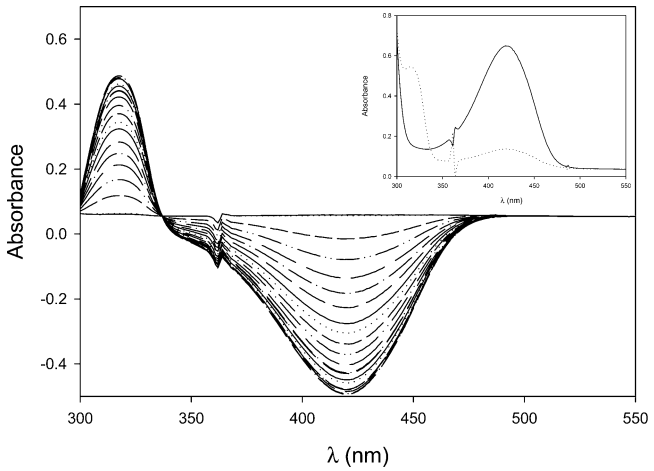

FIGURE 4: Accumulated diode array scans of alanine racemase over a 20 min incubation with D-cycloserine (absorption at 420 nm decreases with a concomitant increase at 318 nm). Inset: wavelength scan of alanine racemase before (solid line, t_0) and after (dotted line, t_f) addition of D-cycloserine. Scans for L-cycloserine appear similar (not shown).

the mechanism in the two-base *B. stearothermophilus* alanine racemase system.

Kinetics of Inactivation. PLP-dependent enzymes have several characteristic absorption maxima dependent upon the form of bound cofactor (Scheme 1), which allow chemical differentiation between the potential adducts generated upon substrate binding (*22*). Spectral analyses of native *B. stearothermophilus* alanine racemase show an absorption peak at 420 nm (Figure 4 inset, t_0 scan), indicative of bound pyridoxal in an aldimine linkage. Upon formation of a saturated C4′ carbon on the cofactor, such as occurs in PMP, the absorption maximum shifts approximately 100 nm downfield to 320 nm (*22*). This phenomenon was observed upon incubation of alanine racemase with either enantiomer of cycloserine (Figure 4 inset, t_f scan). There is a clear decrease in absorbance at 420 nm with a concomitant increase at 318 nm, yielding an isosbestic point at 337 nm (Figure 4). The changes in absorbance at 420 nm upon incubation with L- or D-cycloserine follow first-order kinetics (Figures 5 and 6, respectively). Analysis of these data according to eq 1 (inset, Figures 5 and 6) generates the rate constants presented in Table 2.

The shift in absorption maximum upon incubation of alanine racemase with cycloserine (Figure 4) supports the structural observation of internal aldimine conversion to cofactor saturated at C4′ (i.e., transimination) (*22*). While this defines some of the chemical species in the inactivation pathway, a number of intermediates proposed have similar or identical absorption spectra and cannot be individually distinguished. Thus, the changes in absorbance maxima of various PLP species, while monitoring cofactor chemistry, do not directly yield a quantitative measure of enzyme inactivation. To establish these rates, Figures 7 and 8 show the time-dependent inactivation of alanine racemase after incubating the enzyme with varying concentrations of either isomer of cycloserine and determining the percentage of remaining activity as a function of time. The inactivation rates derived from the double reciprocal plots (inset, Figures 7 and 8) according to eq 1 are presented in Table 2.

Both the rate in absorbance loss at 420 nm (Figures 5 and 6) and the time-dependent inactivation analysis (Figures 7 and 8, summarized in Table 2) of alanine racemase by L- and D-cycloserine show a significant difference in rates between the two enantiomers, an observation not uncommon to inhibitors of alanine racemase in general (*8*). This disparity must be due to a difference in the first irreversible step k_2 as in eq 1. This suggests two different inactivation pathways for the two isomers with an order of magnitude difference in rate between them. Previous theories speculated that both isomers bound in similar orientations, resulting in steric hindrance of one enantiomer. However, the two base mechanism does not lend support to this hypothesis (*4*, *5*, *8*, *23*).

In comparison to the time-dependent inactivation studies, the spectral changes at 420 nm occur at a faster rate (Table 2). While the difference is slight (3−6-fold), this indicates

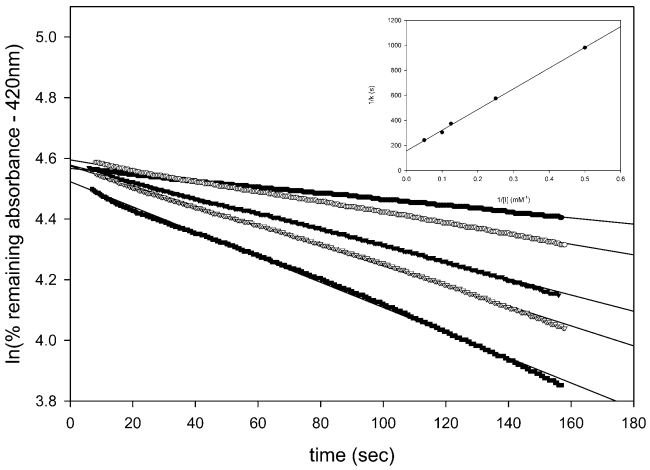

FIGURE 5: Time dependent loss of absorbance at 420 nm upon incubation of alanine racemase with 2 (●), 4 (○), 8 (▼), 10 (▽), and 20 mM (■) L-cycloserine. Inset: double reciprocal plot.

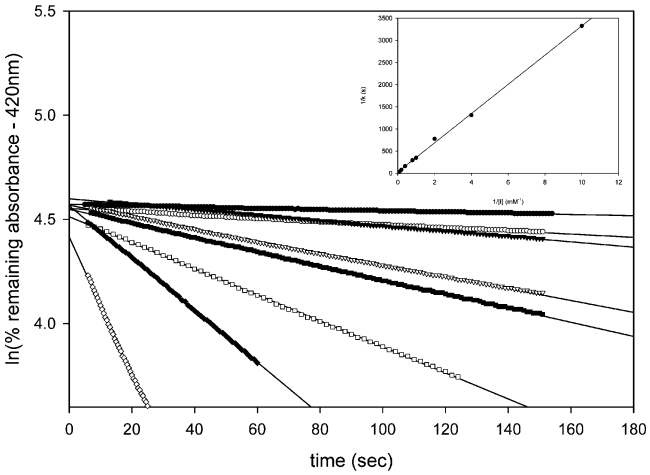

FIGURE 6: Time-dependent loss of absorbance at 420 nm upon incubation of alanine racemase with 0.1 (●), 0.25 (○), 0.5 (▼), 1.0 (▽), 1.25 (■), 2.5 (□), 5 (◆), and 10 mM (◇) D-cycloserine. Inset: double reciprocal plot.

Table 2: Kinetic Parameters for Cycloserine with Alanine Racemase[a]

	DCS		LCS	
measured parameter	$k_2 \times 10^{-3}$	K_i (app)	$k_2 \times 10^{-3}$	K_i (app)
Δ420 nm	36 ± 23	12 ± 0.2	6.4 ± 0.4	11 ± 0.2
enzyme inactivation	16 ± 10	0.13 ± 0.01	0.92 ± 0.13	0.08 ± 0.01

[a] Where k_2 is the rate (mM s^{-1}) and K_i(app) is (k_{-1}/k_1) from eq 1.

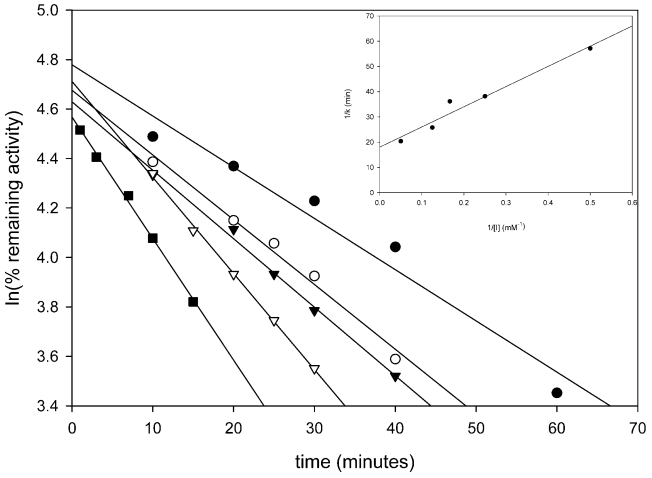

FIGURE 7: Time-dependent inactivation of alanine racemase upon incubation with 2 (●), 4 (○), 6 (▼), 8 (▽), and 20 mM (■) L-cycloserine. Inset: double reciprocal plot.

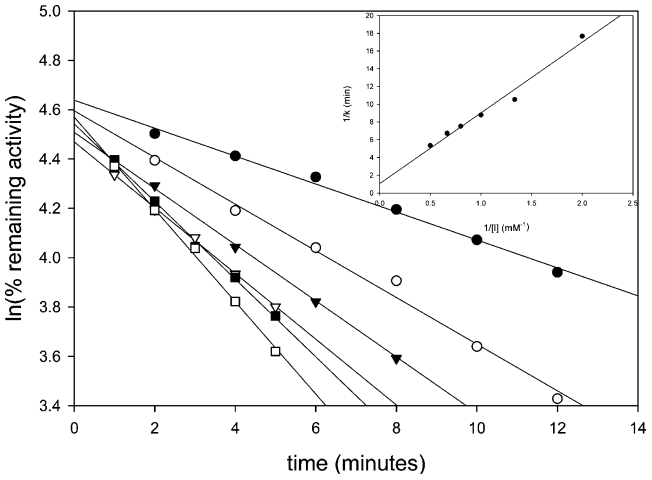

FIGURE 8: Time-dependent inactivation of alanine racemase upon incubation with 0.5 (●), 0.75 (○), 1.0 (▼), 1.25 (▽), 1.5 (■), and 2.0 mM (□) D-cycloserine. Inset: double reciprocal plot.

the potential for reversibility upon loss of the aldimine linkage. Therefore, inactivation of alanine racemase by cycloserine must rely upon the formation of the stable isoxazole resulting from the final tautomerization.

The K_i(app) values determined from inactivation kinetics must be taken with caution, as such K_i values may differ from those derived directly from competitive inhibition kinetics (*24*). Nonetheless, if we assume that the K_i(app) values for the spectral studies at 420 nm represent the true K_i (if the mechanism in Scheme 1 holds for alanine racemase, vide infra), then the rate of inactivation (k_2 in eq 1) approaches the K_i for the D-enantiomer (Table 2). In such a case, saturation kinetics may be difficult to observe, borne out as large errors such as those given for the D-isomer in Table 2.

Racemization of Cycloserine. To determine whether cycloserine undergoes any detectable enzyme-catalyzed racemization, circular dichroism studies were performed. Incubation of alanine racemase with either isomer of alanine shows rapid equilibration within one minute (data not shown). However, experiments utilizing either enantiomer of cycloserine show slight to negligible racemization within the linear range of the instrument over a period of 15 min and only at higher concentrations of enzyme. Nonetheless,

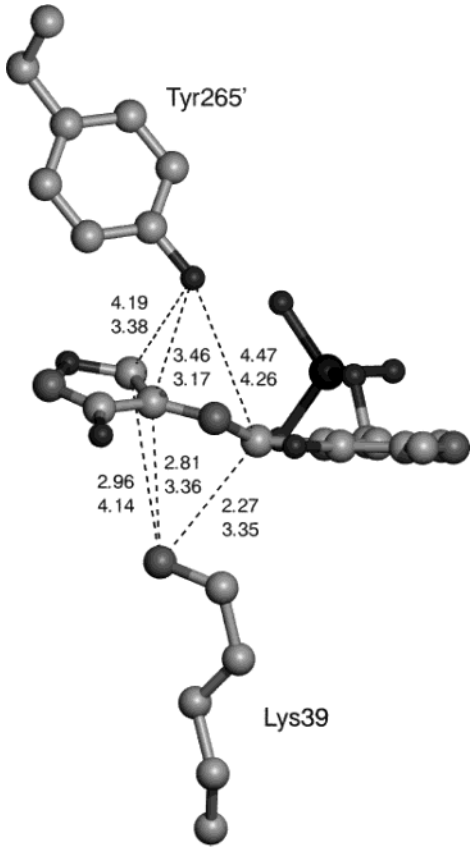

FIGURE 9: Final model of the 3-hydroxyisoxazole PMP derivative (derived from L-cycloserine). Distances are shown (Å) for the L-/D-isomer from either Lys39 or Tyr265 to the C_β, C_α, or C4′ on the isoxazole. Prime labels indicate residues donated by the other subunit in the dimer.

racemization of cycloserine is certainly possible on the enzyme without release of the enantiomer before transimination occurs, and therefore cannot be ruled out in mechanisms which describe its inactivation pathway.

Mechanism of Inactivation. Cycloserine inactivation requires two prototropic shifts, one in which transimination occurs and a second which forms the stable isoxazole. In the aldimine to ketimine (i.e., transimination) conversion step, the crystallographic experiments offer a possible candidate for proton transfer in the case of both cycloserine isomers. While either Tyr265 or Lys39 can deprotonate the α-carbon of substrate, the phenolic oxygen of Tyr265 sits 4.5 Å from the C4′ carbon on the isoxazole ring of L-cycloserine (Figure 9). At these distances, it seems unlikely that Tyr265 could act as an acid or base, though it is conceded that this structure may not accurately represent the distances that exist between these atoms during the course of the reaction. Under these circumstances, the C4′ atom, and therefore the entire cofactor, would need to move toward Tyr265 by more than 1 Å. Further, no manual torsioning of the side chain is possible to permit the phenolic oxygen of Tyr265 to come within the distances typically required for acid−base chemistry. On the other hand, Lys39 is 2.3 Å from C4′ in the same structure, a reasonable distance for proton transfer. The second prototropic shift is unclear, as Tyr265 varies between 3.0 and 4.2 Å from the β-carbon of cycloserine, while Lys39 is between 3.0 and 4.1 Å from the same atom (Figure 9).

Therefore, we suggest two possibilities outlined in Scheme 2 to explain the differences in inactivation rates and identical

Scheme 2: Proposed Mechanism of Inactivation for Alanine Racemase by Cycloserine[a]

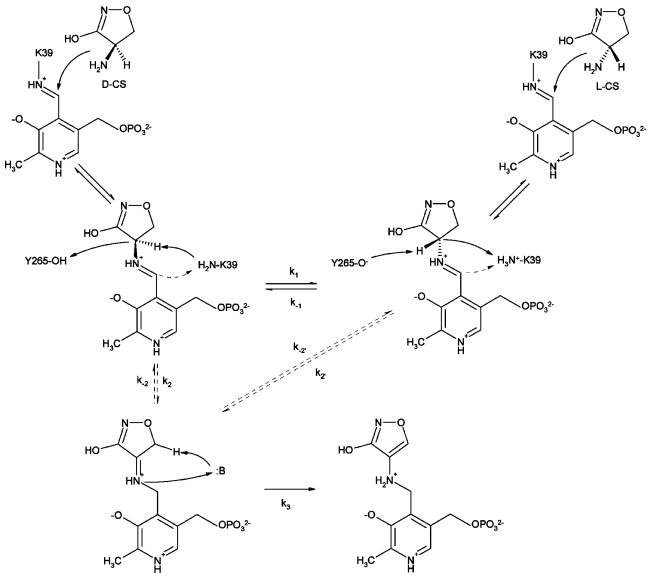

[a] Proton transfers are drawn as concerted mechanisms for the sake of brevity.

structural results. The first requires L- to D-cycloserine racemization before inactivation can take place (k_{-1}). The subsequent aldimine to ketimine conversion (k_2) invokes Lys39, as it is in the correct position and orientation for the required 1,3-prototropic shift. The resulting differences in rates between L- and D-cycloserine are a result of the additional racemization step that would be necessary in the case of L-cycloserine. For this to be true, racemization (at least in the L to D direction) must be presumably slow in relation to transimination. Additionally, the apparent lack of racemization suggests that k_2 must be fast in relation to dissociation of inhibitor. The second possibility has the internal aldimine species passing through two separate transimination pathways depending upon the initial stereochemistry of the inhibitor (rates k_2 and $k_{2'}$ in Scheme 2). The D-cycloserine pathway (k_2) utilizes Lys39 in a dual role as both acid and base. In the L-isomer case ($k_{2'}$), Tyr265 acts in the initial deprotonation of the α-carbon, leading to protonation on the C4′ position by Lys39. For this scheme to agree with the determined (first order) inactivation rates and apparent lack of racemization, $k_{2'}$ must be slower than k_2 and faster than k_{-1}. This can be rationalized if Tyr265 abstracts the C_α proton of the L-isomer, leaving Lys39 in the incorrect protonation state (pK_a ~7.3) to effectively reprotonate C4′ on the cofactor, thereby resulting in the observed rate decrease in $k_{2'}$ versus k_2 (*5*).

On the basis of the evidence suggesting that the change in absorbance (corresponding to loss of the aldimine with concomitant increase in the ketimine species) is faster than actual enzyme inactivation, all of the steps leading up to ketimine formation can be considered reversible. Although this ketimine product is the same for each isomer, the K_i(app) values and rates of inactivation show a marked difference (Table 2), indicating different rate limiting steps that cannot arise solely due to a single step (represented by k_2) as per eq 1. Therefore, eq 1 must be modified such that k_2 (from eq 1) consists of (at a minimum) two steps, as indicated in eq 2:

$$E + I \underset{k_{-1}}{\overset{k_1}{\rightleftharpoons}} E{\cdot}I \underset{k_{-2}}{\overset{k_2}{\rightleftharpoons}} E{\cdot}I^* \xrightarrow{k_3} E{\cdot}X \qquad (2)$$

Here, the measured inactivation rates are then a combination of inactivation (k_3) and the prior conversion from E·I to E·I* (k_2). For this to hold given the kinetic evidence thus far, one of two possibilities can occur. Transimination (represented by k_2 in eq 2) may be fast in relation to inactivation (k_3), such that the inactivation rates represent intrinsic differences in k_2 for the two isomers. Alternatively, transimination may be slow in the L-isomer case and fast with the D-isomer, such that the inactivation rates reflect a change in the rate-limiting step from k_2 to k_3. A slow inactivation step seems reasonable given the lack of an obvious acid for proton donation (Figure 9, represented as B in Scheme 2), and therefore no assignment of its character is made in the proposed scheme.

The results from these inactivation studies of *B. stearothermophilus* alanine racemase by cycloserine have implications for the racemization mechanism. Specifically, alanine racemase must control the cofactor to promote racemization over transamination with substrate. This study has shown that Lys39 is capable of both proton abstraction and transfer (particularly between substrate C_α and cofactor C4′). While the latter case leads to transamination (supporting earlier studies suggesting this possibility (*11*)), alanine racemase uses Tyr265 in a diametrically opposed fashion that favors the former reaction.

ACKNOWLEDGMENT

We thank Todd Holyoak for helpful discussions, experimental questions, and critical reading of the manuscript. Michael Toney and Michael Spies provided assistance with the circular dichroism experiments and offered additional discussions. We also thank Lizbeth Hedstrom for use of the diode array spectrophotometer.

REFERENCES

1. Mathews, C. K., and van Holde, K. E. (1996) *Biochemistry*, Benjamin/Cummings, Menlo Park, CA.
2. Adams, E. (1976) *Adv. Enzymol. Relat. Areas Mol. Biol. 44*, 69−138.
3. John, R. A. (1995) *Biochim. Biophys. Acta 1248*, 81−96.
4. Stamper, G. F., Morollo, A. A., and Ringe, D. (1998) *Biochemistry 37*(29), 10438−10445.
5. Sun, S., and Toney, M. D. (1999) *Biochemistry 38*(13), 4058−4065.
6. Johnston, R. B., Scholz, J. J., Diven, W. F., and Shephard, S. (1968) in *Pyridoxal Catalysis: Enzymes and Model Systems* (Snell, E. E., Braunstein, A. E., Severin, E. S. and Torchinsky, Y. M., Eds.) pp 537−547, John Wiley & Sons, New York.
7. Soper, T. S., and Manning, J. M. (1981) *J. Biol. Chem. 256*, 4263−4268.
8. Wang, E., and Walsh, C. (1978) *Biochemistry 17*(7), 1313−1321.
9. Peisach, D., Chipman, D. M., van Ophem, P. W., Manning, J. M., and Ringe, D. (1998) *J. Am. Chem. Soc. 120*, 2268−2274.
10. Malashkevich, V. N., Strop, P., Keller, J. W., Jansonius, J. N., and Toney, M. D. (1999) *J. Mol. Biol. 294*, 193−200.
11. Kurokawa, Y., Watanabe, A., Yoshimura, T., Esaki, N., and Soda, K. (1998) *J. Biochem. 124*(6), 1163−1169.
12. Kirsch, J. F., Apicella, C., and Handel, T. (1999) in *Enzymatic Mechanisms* (Frey, P. A., and Northrop, D. B., Eds.) pp 198−203, IOS Press, Washington, DC.
13. Watanabe, A., Yoshimura, T., Mikami, B., Hayashi, H., Kagamiyama, H., and Esaki, N. (2002) *J. Biol. Chem. 277*(21), 19166−19172.

14. Morollo, A. A., Petsko, G. A., and Ringe, D. (1999) *Biochemistry 38*(11), 3293−3301.
15. Shaw, J. P., Petsko, G. A., and Ringe, D. (1997) *Biochemistry 36*(6), 1329−1342.
16. Otwinowski, W., and Minor, W. (1997) *Methods Enzymol. 276*, 307−326.
17. Brünger, A. T., Adams, P. D., Clore, G. M., Delano, W. L., Gros, P., Grosse-Kunstlever, R. W., Jiang, J. S., Kuszeqski, J., Nilges, N., Pannu, N. S., Read, R. J., Rice, L. M., Simonson, T., and Warren, G. L. (1998) *Acta Crystallogr. D54*, 905−921.
18. Read, R. (1986) *Acta Crystallogr. A42*, 140−149.
19. Kleywegt, G. J., and Brünger, A. T. (1996) *Structure 4*, 897−904.
20. Hodel, A., Kim, S. H., and Brünger, A. T. (1992) *Acta Crystallogr. A48*, 851−859.
21. Watanabe, A., Yoshimura, T., Mikami, B., and Esaki, N. (1999) *J. Biochem. 126*, 781−786.
22. Kallen, R. G., Korpela, T., Martell, A. E., Matsushima, Y., Metzler, C. M., Metzler, D. E., Morozov, Y. V., Ralston, I. M., Savin, F. A., Torchinsky, Y. M., and Ueno, H. (1985) in *Transaminases* (Christen, P., and Metzler, D. E., Eds.) Vol. 2, pp 37−108, John Wiley & Sons, New York.
23. Ondrechen, M. J., Briggs, J. M., and McCammon, J. A. (2001) *J. Am. Chem. Soc. 123*(12), 2830−2834.
24. Plapp, B. V. (1982) in *Contemporary Enzyme Kinetics and Mechanism* (Purich, D. L., Ed.) pp 321−352, Academic Press Inc., Orlando, FL.
25. Brünger, A. T. (1992) *Nature 355*, 472−475.

BI027022D